LASER FUNCTIONALIZATION OF MEDICAL SILICONE SURFACE MICROSTRUCTURE AND INVESTIGATION OF ITS ANISOTROPIC TRIBOLOGICAL PROPERTIES

Adam Patalas[1*], Mariusz Winiecki[2*], Paweł Zawadzki[1], Ryszard Uklejewski[2]

[1] Institute of Mechanical Technology, Poznan University of Technology, Piotrowo 3, 60-965 Poznan, Poland
[2] Department of Constructional Materials and Biomaterials, Faculty of Materials Engineering, Kazimierz Wielki University, Jan Karol Chodkiewicz Street 30, 85-064 Bydgoszcz, Poland
*e-mail: adam.patalas@put.poznan.pl; winiecki@ukw.edu.pl

Abstract

In this study, the assessment of the possibility of imparting anisotropic tribological properties to medical silicone surfaces using laser surface texturing was performed. The transversal-shaped microgrooves were laser-textured on the surface of the silicone samples applying different angles of incidence of the laser beam (α) ranging from 0° to 40°. The surface characteristics of the laser-textured silicone surface were performed by optical microscopy, surface 3D topography measurements, and contact angle measurements; the tribological tests were carried out under technically dry friction conditions and friction with lubrication conditions. The results showed: a significant increase in surface texture parameters values with Sq values ranging from 7.57 μm for α = 0° to 36.9 μm for α = 10°, compared to the non-textured sample 1.52 μm, increased hydrophilicity of the textured surfaces for most samples demonstrated by contact angle measured values for α = 0° sample showing the largest contact angle 126° as compared to the non-textured samples 103°. The produced anisotropic microstructure of the textured silicone surface, i.e. its directionality, is evidenced by obtained values of the texture aspect ratio (Str) tending to 0.00 for all textured samples. Changes in the friction coefficient's directionality in the forward and backward directions were noted for α values above 20° for both dry conditions and friction with lubrication conditions. We can conclude that laser surface texturing allows for the effective functionalization of a medical silicone surface in terms of the anisotropy of its tribological properties.

Keywords: *silicone, laser surface texturing, laser surface functionalization, friction, anisotropic tribological properties*

Introduction

Silicones, also known as polysiloxanes, are organosilicon polymers that have found widespread and diverse applications for medical and implantable devices since the 1940s [1]. It is due to their superior biocompatibility with multiple components, compatibility with many sterilization methods, resistance to repeated sterilization and biodurability when interacting with host tissues [2,3]. In terms of physicochemical properties beneficial for their use in the medical field are silicones' excellent chemical inertness and thermostability, hydrophobicity, low surface energy, appropriate mechanical properties (modulus and stretchability) with durability and ease of moulding by many methods [4-6]. Silicones are versatile and can be formulated into various forms, such as silicone elastomer, silicone gel, or silicone adhesive, which determines their intended applications. Medical applications of silicones include, but are not limited to, contact lenses [7], breast implants [8], drains [9,10] and shunts [11], catheters [12], reconstructive gel fillers [13] and sheeting [14], cranio-maxillo-facial implants [15,16], scaffolds for nerve regeneration [17], and implants for small joint arthroplasty [18], as well as for devices with a non-silicone substrate that had been silicone-coated to provide less host reaction, such as needles, syringes, or blood collection vials.

The working surfaces of the material often require modification that gives them specific properties determined by the functions they are to perform. Surface functionalization allows for enhancing their performance for example in terms of hydrophilization by increasing their surface wettability [19,20], enhancing the tribological properties of the material, such as load capacity, wear resistance and coefficient of friction [21-24] or modifying the surface properties related to cell/surface interactions i.e., providing the surface topography endorsing tissue/materials integration through cells adhesion and activity [25-28]. The micro- and nanostructural functionalization of the work surface can be performed by many methods such as electric discharge texturing [29], focused ion beams [30], electrochemical machining [31], hot embossing [32], lithography, or mechanical texturing [33]. Laser surface texturing (LST) is a relatively new and widely explored method for acquiring specific physical surface properties desired in functional surfaces that allow surface structuring by producing a defined pattern or texture on a work surface with excellent controllability [34,35].

The aim of the work is to assess the possibility of imparting anisotropic tribological properties to medical silicone surfaces using laser surface texturing.

[Engineering of Biomaterials 171 (2023) 23-29]

doi:10.34821/eng.biomat.171.2023.23-29

Submitted: 2023-11-10, Accepted: 2023-12-11, Published: 2023-12-14

Materials and Methods

Sample surface modification

In this study, medical-grade RTV-2 silicone, approved for skin contact, and designated as SIL 25, was used. It is a two-part mixture for curing silicone at room temperature. Samples in the shape of rectangular prisms measuring 20x60 mm and 4 mm thick were moulded. After moulding, they were degassed using a vacuum pump, followed by curing at a temperature of 50°C for 45 min.

A blue laser (PLH3D-XT-10, Opt Lasers, Warsaw, Poland), with an output power of 0.5 W at 405 nm laser wavelength and square laser spot of 10 µm was used to produce transversal-shaped microgrooves on the surface of the sample. During the microgrooves texturing, the angle of incidence of the laser beam on the sample surface was varied while maintaining a constant power density of 8.8 kW/mm^2, which is approximately 80% of the maximum power density. The power density of the laser beam was selected experimentally, as it ensured the relatively highest repeatability of the texturing results. Depending on the set values angles of incidence of the laser beam on the sample surface of 0°, 10°, 20°, 30°, and 40°, the samples are referred to as LA0, LA10, LA20, LA30 and LA40, while the untextured sample is denoted as Raw. The scheme of geometry of laser-textured surface microgrooves is presented in FIG. 1.

Sample surface characterization

The surface morphology of the textured microgrooves was examined by applying an optical microscope and a 3D profilometry apparatus (PortableRL, Bruker Alicona, Raaba, Austria). The values of the geometric features of the microgrooves were determined. According to the microgrove geometry presented in FIG. 1, the following geometric features were measured: α – deviation of microgroove angle bisector from the normal to the sample surface (°), β – microgroove apex angle (°), d – microgroove depth (µm) and B – the distance between grooves (µm). The surface topography measurements were carried out by the focus-variation method combining an optical system's small depth of focus with vertical scanning to provide topographical and colour information from the focus variation. From the group 3D areal surface texture parameters described in [36,37] the parameters, such as the root mean square roughness (Sq), the maximum pit height (Sv), the texture aspect ratio (Str), skewness (Ssk) and kurtosis (Sku) were selected and measured with a cut-off wavelength of 800 µm. Moreover, the material ratio curves were determined and the valley void volume (Vvv) was evaluated. The accuracy of the measurements in terms of uncertainty was U = 50 nm.

Contact angle measurements on the laser-textured surface using the OCA 15Pro Goniometer (DataPhysics Instruments GmbH, Filderstadt, Germany) equipped with an automatic liquid drop dosing system. The dropping unit was set to the drop dosing volume of 2 µl and the drop dosing rate of 0.5 µl/s. Since Ringer's solution is a recognized SBF, it was used in this study in contact angle measurements [38]. The temperature in the laboratory room during the experiments was stable and amounted to 22.4°C. The static contact angle on a flat surface was calculated with dedicated goniometer software (SCA 20, DataPhysics Instruments GmbH, Filderstadt, Germany) by automatically detecting baselines and tangents. The accuracy of the contact angle measurement is considered ± 0.1°.

The tribological oscillating ball-on-flat tests were carried out using a Universal Mechanical Tester Tribometr (UMT TriboLab™, Billerica, Massachusetts, USA) according to the ASTM G133-22 standard [39]. The tribological tests were carried out under technically dry friction conditions and friction conditions with lubrication with the Ringer's solution, collagen hydrolyzate and silicone oil. The counter-sample as a stainless steel ball with a 10 mm diameter was applied. A surrounding climate chamber kept the environmental conditions constant at a temperature of 24°C ± 1°C and of 40% ± 1% relative humidity. The linear drive was used to apply a reciprocating movement of the velocity up to 10 mm/s, and a linear sliding length was set for 30 mm. The applied forces were controlled by sensors' module DFM-20 (UMT TriboLab™, Billerica, Massachusetts, USA) within the range of 0.2 N to 20 N and the contact force was set to 5 N ± 0.2 N.

Results and Discussion

The microscope images of the side views of textured samples are shown in FIG. 2. The measured values of geometric features of microgrooves laser-textured on a silicone material are provided in TABLE 1. Analyzing the obtained microscope images of the laser-textured microgrooves and their measured geometric features, it can be seen that the set laser beam angle is very close to the deviation of the microgroove angle bisector from the normal to the sample surface. The only significant difference is found for the LA10 sample. The largest groove depth was obtained for the LA10 sample and the smallest for LA0.

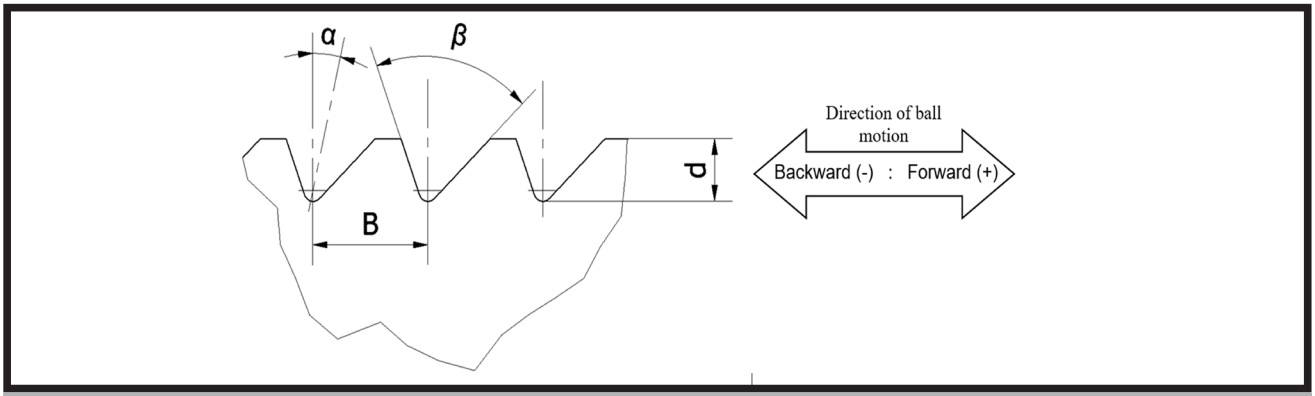

FIG. 1. Design of microgrooves geometry with annotated geometrical features: α – deviation of microgroove apex angle (briefly called also *'microgroove axis'*) bisector from the normal to sample surface (°), β – microgroove apex angle (°), d – microgroove depth (µm), B – distance between microgrooves (µm).

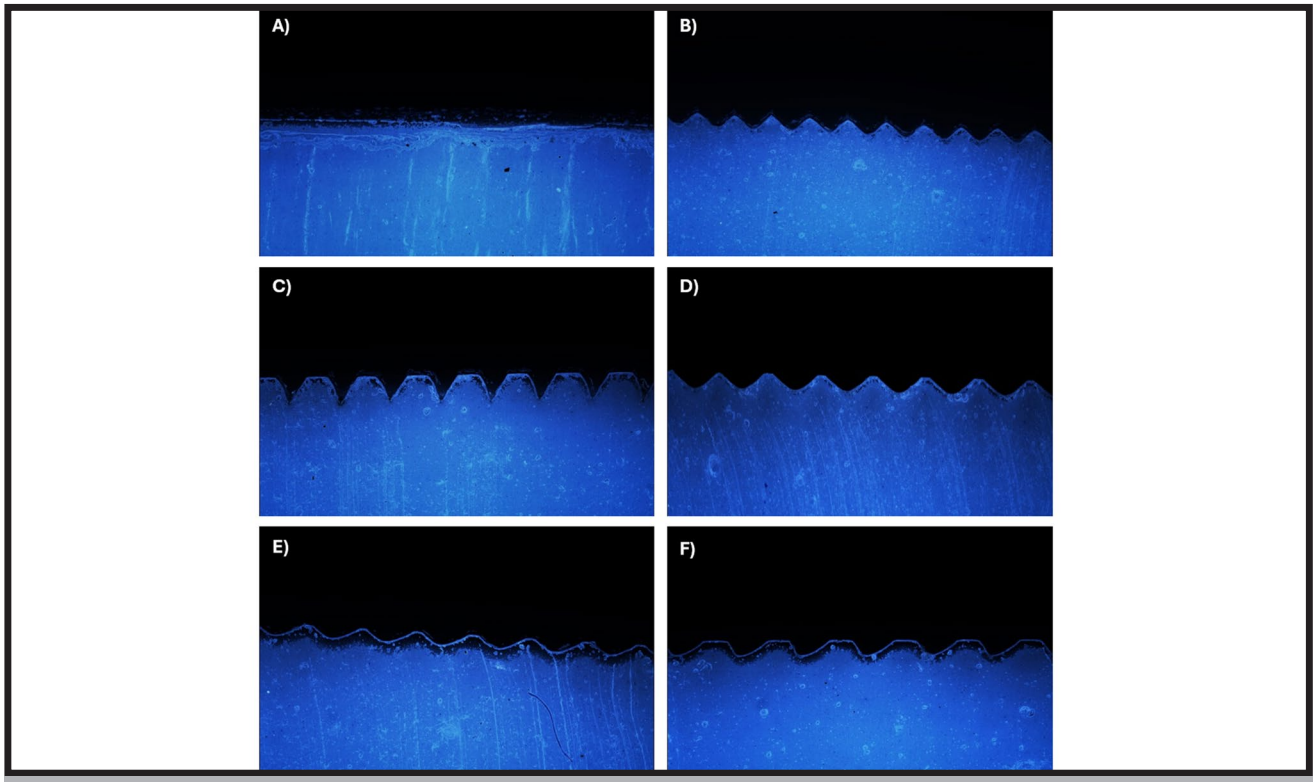

FIG. 2. Side views of laser-textured silicone material: A) Raw, B) LA0, C) LA10, D) LA20, E) LA30, and F) LA40.

TABLE 1. The values of geometric features of microgrooves laser-textured on a silicone material.

Sample	Set angle of laser beam (°)	α (°)	d (µm)	β (°)	B (µm)
LA0	0	0 ± 0	48 ± 4	34 ± 2	195 ± 10
LA10	10	14 ± 1	98 ± 3	41 ± 2	255 ± 8
LA20	20	18 ± 2	89 ± 4	57 ± 1	273 ± 8
LA30	30	30 ± 3	59 ± 4	51 ± 2	286 ± 9
LA40	40	41 ± 2	67 ± 1	59 ± 3	323 ± 9

FIGURE 3 shows the 2D surface topography of the microgrooves laser-textured on the silicone material surface. The material share curves created based on these representative areas are presented in FIG. 4. As it can be seen, a plateau was obtained for samples LA10-LA40. The sharpest groove notches were obtained for sample LA10. The groove notches of the remaining samples are characterized by a gentle valley/end.

In statistical terms, a significant increase in the Sq parameter values was observed due to surface texturization, as intended (TABLE 2). According to the assumptions, there was an increase in the maximum value for the valley's depth, as confirmed by the high values of the parameter Sv. From a tribological perspective, a notable feature is the change in the parameter Ssk value, which shifted from the baseline value of Ssk = -0.63 towards 0 for all surfaces. Consequently, there was an increase in the symmetry of the surface relative to the mean line, along with the kurtosis parameter Sku, which for textured surfaces takes values Sku ≤ 3, confirming the designed periodicity in the resulting surface layer structure. In terms of functional parameters, attention should be paid to Vvv, which increased several times for textured samples, potentially ensuring improvement in friction parameters, particularly in the presence of lubricants from a tribological standpoint. Following the assumptions, a significant directionality of the structure was achieved, which is confirmed by the values of the Str coefficient < 0.03.

The results of the contact angle measurement are presented in TABLE 3 and FIG. 5. The contact angle measurements revealed that the LA10 sample exhibited the largest contact angle. Interestingly, it was observed that the contact angle values for the LA10-40 samples consistently exceeded those of the untextured reference sample. It was not possible to correctly measure the contact angle for the LA0 sample, but as can be seen in FIG. 5A, the droplet spread in the microgrooves. This may be because the measuring liquid – Ringer's liquid, has a viscosity similar to water and did not form a stable drop. The measured one-second contact angle value for LA0 is 86.0 ± 4.9. This disparity in contact angle values between the LA0 sample and the other textured samples may be attributed to the presence of sharp-edged microgrooves in the former, facilitating enhanced drop penetration into the grooves. Conversely, in the textured samples (LA10-40), the limited liquid penetration into the valley spaces is anticipated, largely due to surface tension effects. FIGURE 5 presents the results of measuring the friction coefficient values for different environmental conditions. TABLE 4 presents the percentage increase of the directional coefficient of friction for different samples under various types of lubrication.

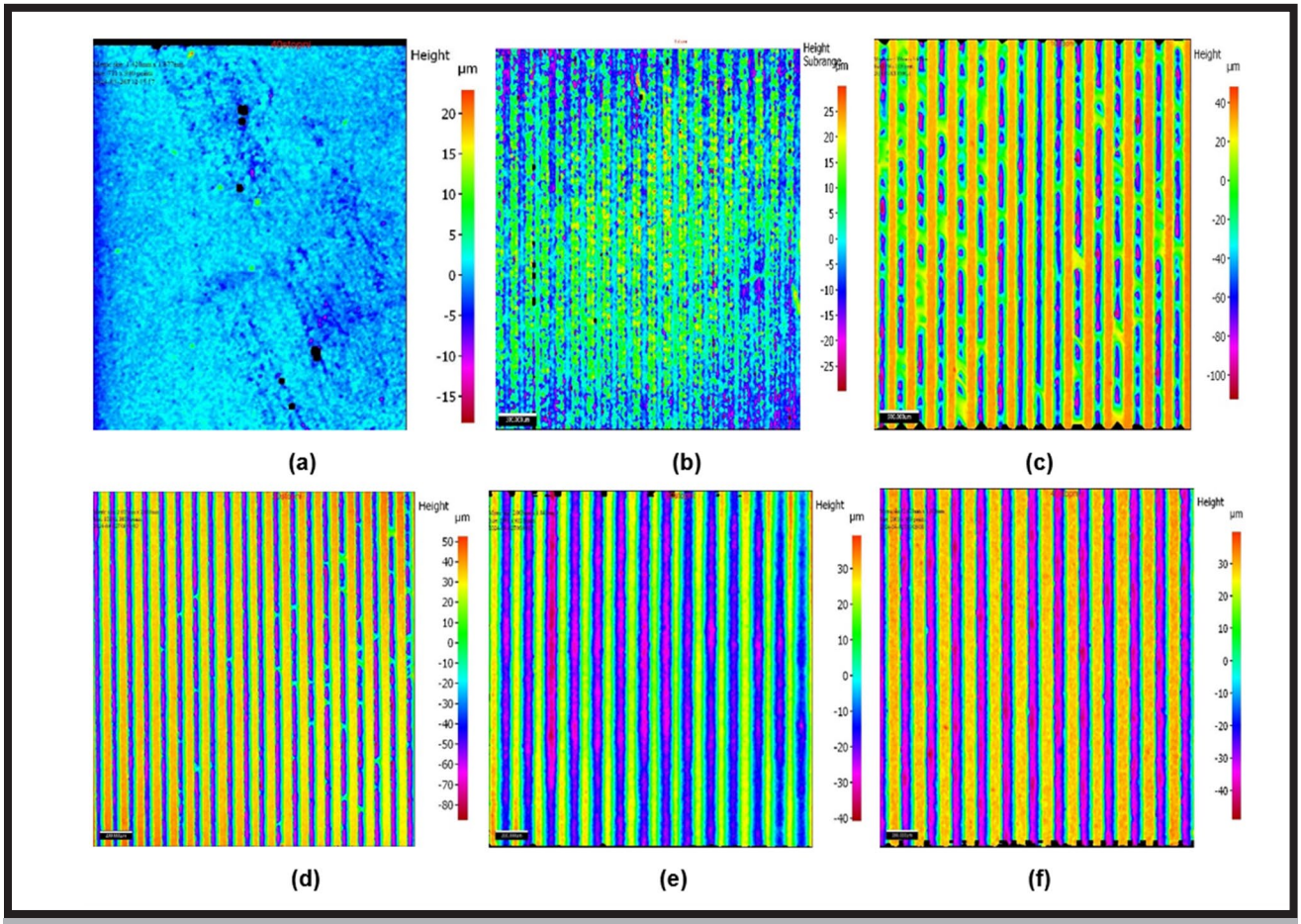

FIG. 3. 2D surface topography of the laser-textured silicone surface samples (left to right): Raw, LA0, LA10 (a-c), and LA20, LA30, LA40 (d-f).

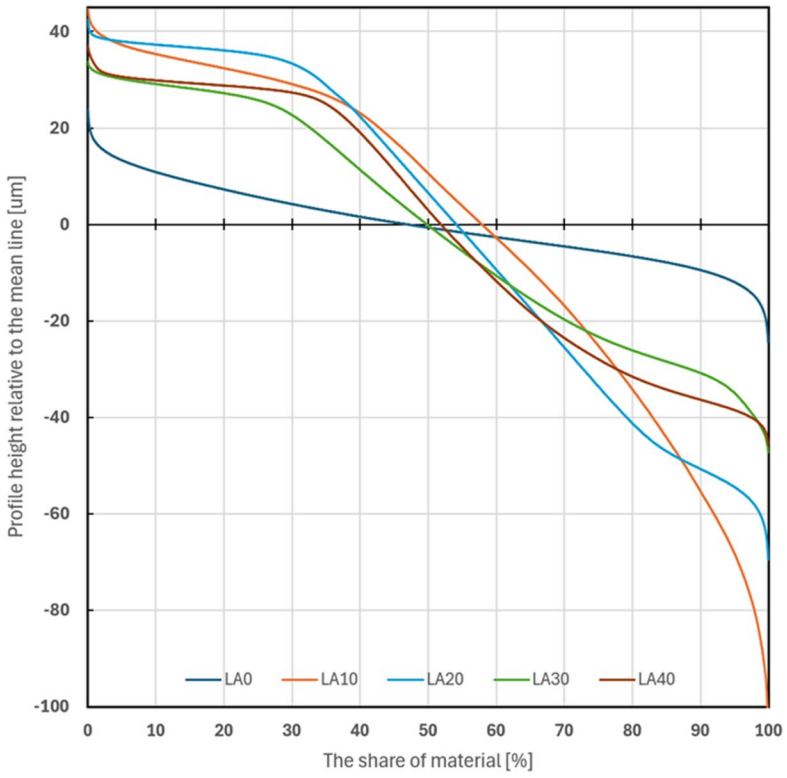

FIG. 4. Material share curves for representative areas of laser-textured silicone surface.

TABLE 2. The surface geometric parameters of the laser-textured silicone surface.

Sample	Raw	LA0	LA10	LA20	LA30	LA40
Sq	1.52	7.57	36.9	33.6	17.6	25.4
Sv	18.3	48.32	92.1	113.6	40.3	52.9
Str	0.38	0.04	0.03	0.03	0.04	0.04
Ssk	-0.63	0.055	-0.49	-0.225	0.204	-0.267
Sku	9.955	3	1.79	1.558	1.7	1.409
Vvv	0.254	1.043	3.06	1.722	0.921	1.052

TABLE 3. Average values of the surface contact angle.

Sample	Raw	LA0	LA10	LA20	LA30	LA40
Contact angle	103 ± 2	86 ± 5*	126 ± 3	124 ± 5	109 ± 3	118 ± 4

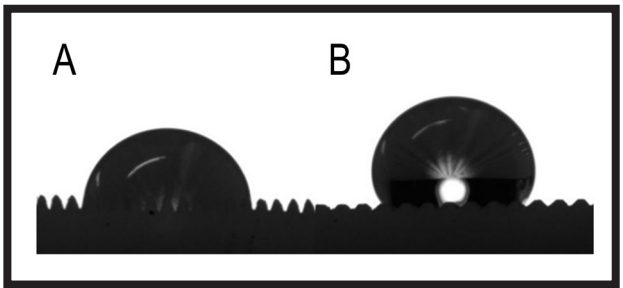

FIG. 5. Example contact angle measurement results: A) LA0, B) LA10.

From the data in FIG. 6, it can be seen that the average friction coefficients range from 0.13 to 1.30. The lowest measured values of the friction coefficient were measured for the combination under silicone oil lubrication conditions. For all measurements, the friction coefficient in the forward direction was lower than in the backward direction. The highest friction coefficient values were for: dry friction – sample LA10, friction in Ringer's fluid – sample LA30, friction in collagen hydrolyzate – sample LA30, friction in silicone oil – sample LA20. For samples tested in a dry environment, it is visible that the largest changes in the friction coefficient value are for samples LA20, LA30, and LA40. For samples tested in the Ringer's fluid and collagen hydrolysate environment, such a significant change was observed only for LA30 and LA40 samples. However, during tests in a silicone oil environment, the largest difference in directional friction coefficient values was observed for samples LA10 and LA20, while for LA10 sample this increase was the largest among all the measurements carried out and it was by 277%; the observed differences in directional friction coefficient values for applied lubricants may be related to different properties of water-based lubricants (Ringer's fluid, collagen hydrolyzate) and non-water-based lubricant (silicone oil).

TABLE 4. Percentage difference of directional coefficient of friction values in forward and backward directions.

Set angle Sample	Lubrication type and percentage increase of directional coefficient of friction			
	Dry	Ringer's fluid	Collagen hydrolyzate	Silicone oil
LA0	27%	11%	76%	22%
LA10	7%	5%	9%	277%
LA 20	114%	13%	7%	176%
LA 30	73%	64%	46%	38%
LA 40	77%	78%	39%	88%

FIGURE 7 compares friction coefficient values as a function of the linear position of the ball counter sample on the tested sample for the LA40 sample and the Raw sample in an oil-lubricated environment. As it can be observed, despite the presence of a lubricating environment (oil), the surface texturization leads to an increase in the friction coefficient values. However, in terms of the directional effect of the textured microstructure, a relatively constant difference between the coefficient of friction value in the forward direction (+) and backward direction (-) is evident.

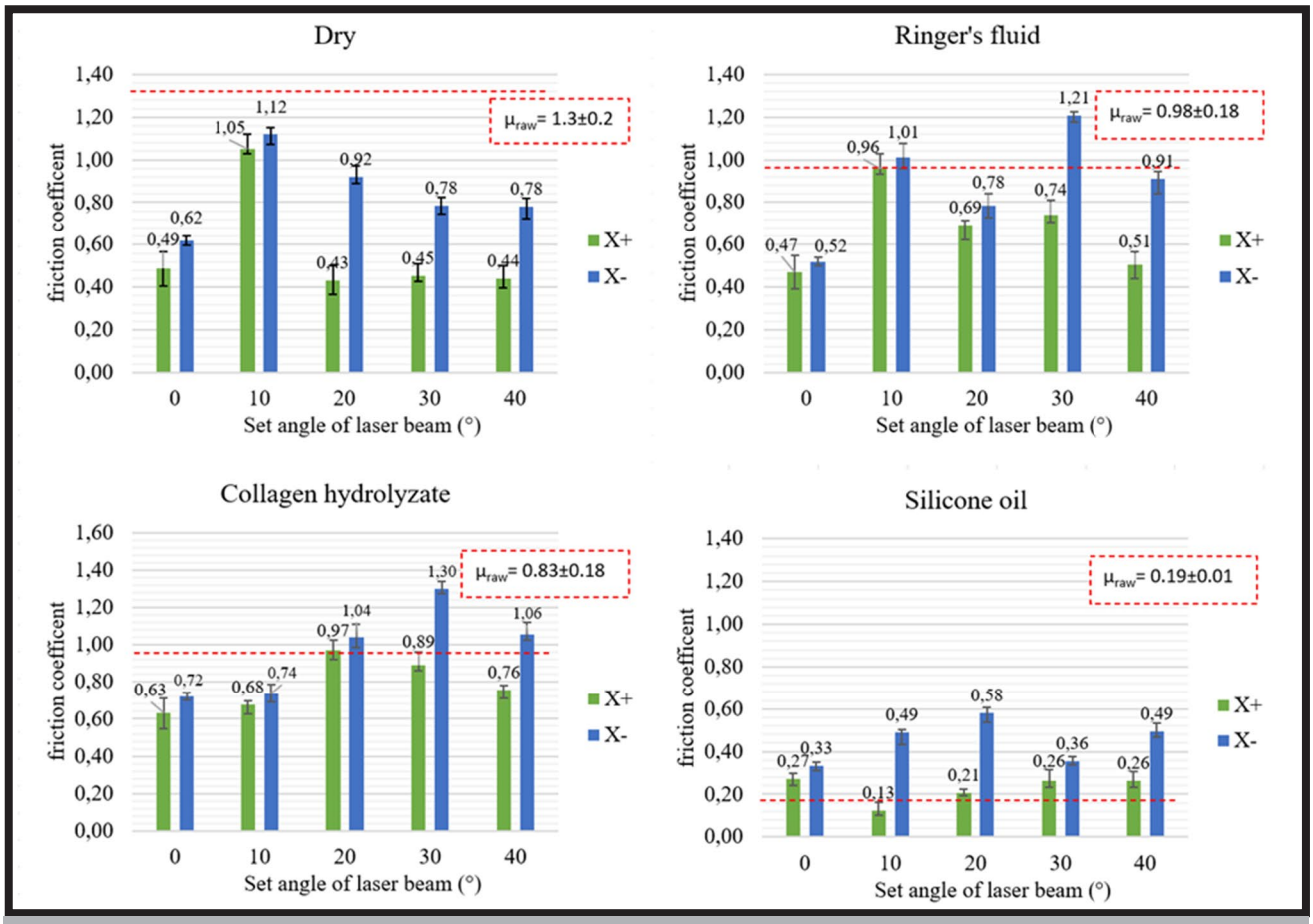

FIG. 6. Results of measuring the directional coefficient of friction values for 4 environmental conditions. Results for unmodified samples are presented as red dashed lines.

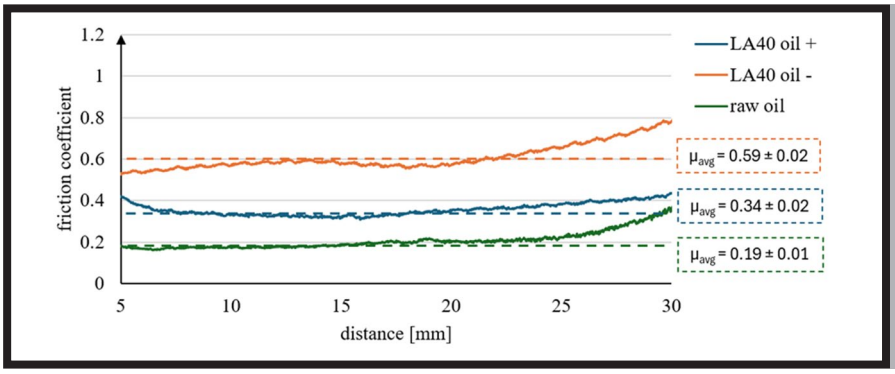

FIG. 7. Comparison of the directional coefficient of friction values as a function of the linear position of the ball counter sample on the tested sample for raw and LA40 textured surfaces in an oil-lubricated environment.

Conclusions and research perspectives

The performed laser texturing of medical silicone surface assures high accuracy of repeatability of surface texture parameters across the textured surface. Produced anisotropic microstructure of the textured silicone surface, i.e. its directionality, is evidenced by the measured values of the texture aspect ratio (Str) tending to 0.00 for all textured samples. The percentage differences in the directional coefficient of friction values registered in forward and backward directions for the laser beam angle setting values above 20° imparts the clearly evident directional anisotropy of the tribological properties of the textured surface.

So, we can conclude that laser surface texturing allows for effective functionalization of medical silicone surface in terms of its directional anisotropy of tribological properties.

Looking forward, future research directions should focus, in our opinion, on exploring the applicability of laser texturing to medical devices with rotationally symmetric elements. Such endeavours hold promise for optimizing the tribological properties of medical devices, thereby enhancing their performance and biocompatibility in clinical settings.

Acknowledgements

This research was funded by the Polish Ministry of Science and Higher Education as a part of an annual subsidy – project numbers: 0614/SBAD/1586.

ORCID iD

A. Patalas: https://orcid.org/0000-0001-5476-6739
M. Winiecki: https://orcid.org/0000-0002-3568-2473
P. Zawadzki: https://orcid.org/0000-0001-8153-8774
R. Uklejewski: https://orcid.org/0000-0002-3587-714X

References

[1] Allen L.V. Jr.: Compounding with Silicones. International Journal of Pharmaceutical Compounding 19(3) (2015) 223-230.
[2] Colas A.R., Curtis J.: Silicone Biomaterials: History and Chemistry & Medical Applications of Silicones. In: Ratner B.D., Hoffman A.S., Schoen F.J., Lemons J.E., Eds): Biomaterials Science: An Introduction to Materials in Medicine. Academic Press; 3rd edition, 2013. 82-91.
[3] Bračič M., Strnad S., Fras Zemljič L.: Silicone in Medical Applications. In: Bioactive Functionalisation of Silicones with Polysaccharides. SpringerBriefs in Molecular Science. Springer, Cham. 2018.
[4] Owen M.J.: Silicone Surface Fundamentals. Macromolecular Rapid Communications 42(5) (2021) e2000360.
[5] Marmo A.C., Grunlan M.A.: Biomedical Silicones: Leveraging Additive Strategies to Propel Modern Utility. ACS Macro Letters 12(2) (2023) 172-182.
[6] Zare M., Ghomi E.R., Venkatraman P.D., Ramakrishna S.: Silicone-based biomaterials for biomedical applications: antimicrobial strategies and 3D printing technologies. Journal of Applied Polymer Science 138(38) (2021) e50969.
[7] Ishihara K., Shi X., Fukazawa K., Yamaoka T., Yao G., Wu J.Y.: Biomimetic-Engineered Silicone Hydrogel Contact Lens Materials. ACS Applied Bio Materials 6(9) (2023) 3600-3616.
[8] Chao A.H., Garza R. 3rd, Povoski S.P.: A review of the use of silicone implants in breast surgery. Expert Review of Medical Devices 13(2) (2016) 143-156.
[9] Bakoš M., Kuťka M.: Drainage in Abdominal Surgery. Biomedical Journal of Scientific & Technical Research 2022 43(3) BJSTR. MS.ID.006912.
[10] Makama J.G., Ameh E.A.: Surgical drains: what the resident needs to know. Nigerian Journal of Medicine 17(3) (2008) 244-250.
[11] Srinivas D., Tyagi G., Singh G.J.: Shunt Implants - Past, Present and Future. Neurology India 69(Supplement) (2021) S463-S470.
[12] Lawrence E.L., Turner I.G.: Materials for urinary catheters: a review of their history and development in the UK. Medical Engineering & Physics 27(6) (2005) 443-453.
[13] Spiera R.F., Gibofsky A., Spiera H.: Silicone gel filled breast implants and connective tissue disease: an overview. Journal of Rheumatology 21(2) (1994) 239-245.
[14] Tian F., Jiang Q., Chen J., Liu Z.: Silicone gel sheeting for treating keloid scars. Cochrane Database of Systematic Reviews 1(1) (2023) CD013878.
[15] Ariani N., Visser A., van Oort R.P., Kusdhany L., Rahardjo T.B., Krom B.P., van der Mei H.C., Vissink A.: Current state of craniofacial prosthetic rehabilitation. International Journal of Prosthodontics 6(1) (2013) 57-67.
[16] Kumar A., Seenivasan M.K., Inbarajan A.: A Literature Review on Biofilm Formation on Silicone and Poymethyl Methacrylate Used for Maxillofacial Prostheses. Cureus 13(11) (2021) e20029.
[17] Yi S., Xu L., Gu X.: Scaffolds for peripheral nerve repair and reconstruction. Experimental Neurology 319 (2019) 112761.
[18] Moran S.L., Rizzo M.: Managing Difficult Problems in Small Joint Arthroplasty: Challenges, Complications, and Revisions. Hand Clinics 39(3) (2023) 307-320.
[19] Pereira R.S., Moura C.G., Henriques B., Chevalier J., Silva F.S., Fredel M.C.: Influence of laser texturing on surface features, mechanical properties and low-temperature degradation behavior of 3Y-TZP. Ceramics International 46 (2020) 3502-3512.
[20] Yu Z., Yang G., Zhang W., Hu J.: Investigating the effect of picosecond laser texturing on microstructure and biofunctionalization of titanium alloy. Journal of Materials Processing Technology 255 (2018) 129-136.
[21] Mao B., Arpith Siddaiah Y.L., Pradeep L.M.: Laser surface texturing and related techniques for enhancing tribological performance of engineering materials: A review. Journal of Manufacturing Processes 53 (2020) 153-173.
[22] Wang C., Li Z., Zhao H., Zhang G., Ren T., Zhang Y.: Enhanced anticorrosion and antiwear properties of Ti-6Al-4V alloys with laser texture and graphene oxide coatings. Tribology International 152 (2020) 106475.
[23] Wu Z., Bao H., Xing Y., Liu L.: Tribological characteristics and advanced processing methods of textured surfaces: A review. International Journal of Advanced Manufacturing Technology 114 (2021) 1241-1277.
[24] Bonse J., Kirner S.V., Griepentrog M., Spaltmann D., Krüger J.: Femtosecond Laser Texturing of Surfaces for Tribological Applications. Materials 11(5) (2018) 801.
[25] Tiainen L., Abreu P., Buciumeanu M., Silva F., Gasik M., Guerrero R.S., Carvalho O.: Novel laser surface texturing for improved primary stability of titanium implants. Journal of the Mechanical Behavior of Biomedical Materials 98 (2019) 26-39.
[26] Shukla P., Waugh D.G., Lawrence J., Vilar R.: Laser surface structuring of ceramics, metals and polymers for biomedical applications: A review. In Laser Surface Modification of Biomaterials; Woodhead Publishing: Cambridge, UK, 2016; pp. 281-299.
[27] Cunha W., Carvalho O., Henriques B., Silva F.S., Özcan M., Souza J.C.M.: Surface modification of zirconia dental implants by laser texturing. Lasers in Medical Science 37(1) (2022) 77-93.
[28] Han J., Zhang F., Van Meerbeek B., Vleugels J., Braem A., Castagne S.: Laser surface texturing of zirconia-based ceramics for dental applications: A review. Materials Science & Engineering C: Materials for Biological Applications 123 (2021) 112034.
[29] Jithin S., Joshi S.S.: Surface topography generation and simulation in electrical discharge texturing: A review. Journal of Materials Processing Technology 298 (2021) 117297.
[30] Kawasegi N., Ozaki K., Morita N., Nishimura K., Yamaguchi M.: Development and machining performance of a textured diamond cutting tool fabricated with a focused ion beam and heat treatment. Precision Engineering 47 (2017) 311-320.
[31] Patel D.S., Jain V.K., Shrivastava A., Ramkumar J.: Electrochemical micro texturing on flat and curved surfaces: simulation and experiments. International Journal of Advanced Manufacturing Technology 100 (2019) 1269-1286.
[32] Pettersson U., Jacobson S.: Tribological texturing of steel surfaces with a novel diamond embossing tool technique. Tribology International 39(7) (2006) 695-700.
[33] Costa H., Hutchings I.: Some innovative surface texturing techniques for tribological purposes. Proceedings of the Institution of Mechanical Engineers, Part J: Journal of Engineering Tribology. 229(4) (2015) 429-448.
[34] Shivakoti I., Kibria G., Cep R., Pradhan B.B., Sharma A.: Laser Surface Texturing for Biomedical Applications: A Review. Coatings 11 (2021) 124.
[35] Moskal D., Martan J., Honner M.: Scanning Strategies in Laser Surface Texturing: A Review. Micromachines 14 (2023) 1241.
[36] Stout K.J., Sullivan P.J., Dong W.P., Mainsah E., Lou N., Mathia T., Zahouani H.: The Development of Methods for The Characterisation of Roughness in Three Dimensions, Report EUR 15178 EN, European Commission, Brussels, 1993, ISBN 0-7044-1313-2
[37] ISO 25178-2:2021. Geometrical product specifications (GPS) — Surface texture: Areal — Part 2: Terms, definitions and surface texture parameters.
[38] Agathopoulos S., Nikolopoulos P.: Wettability and interfacial interactions in bioceramic-body-liquid systems. J Biomed Mater Res. Apr;29(4):421-9 (1995). doi: 10.1002/jbm.820290402.
[39] ASTM G133-22. Standard Test Method for Linearly Reciprocating Ball-on-Flat Sliding Wear.